Protein-Transition Metal Ion Networks

Justin R. Barone,[1*] Kirsten L. Dangaran,[2] Walter F. Schmidt[1]

[1]*Environmental Management and By-Products Utilization Laboratory and Dairy Processing and Products Research Unit, Agricultural Research Service, U.S. Department of Agriculture, Beltsville, Maryland 20705*
[2]*Wyndmoor, Pennsylvania 19038*

Received 30 October 2006; accepted 6 March 2007
DOI 10.1002/app.26654
Published online 16 July 2007 in Wiley InterScience (www.interscience.wiley.com).

ABSTRACT: Proteins obtained from agricultural sources were blended with divalent metal ions to see if binding reactions occurred between protein chains. Feather keratin, egg albumin, and wheat gluten showed elastic modulus increases of 2–3 times with addition of divalent transition metal ions Cu^{2+} and Zn^{2+}. Increasing concentrations of ions resulted in increased stiffness. Birefringence experiments performed concurrently with tensile experiments showed refractive index changes indicative of network formation. Binding divalent alkaline earth metal Ca^{2+} ions did not result in an elastic modulus increase. Addition of Zn^{2+} to egg albumin resulted in a 34% decrease in water permeability but no change in oxygen permeability. FTIR spectroscopy showed that the directed valence of the transition metals was primarily binding glycerol and amide sites on the protein and secondarily carbonyl sites on the protein. © 2007 Wiley Periodicals, Inc. J Appl Polym Sci 106: 1518–1525, 2007

Key words: proteins; metal–polymer complexes; mechanical properties; Fourier transform infrared spectroscopy

INTRODUCTION

There has been much interest over the years in utilizing agriculturally derived polymers in commodity plastics applications, such as packaging. Agriculturally derived polymers would be sustainable and typically biodegradable and therefore advantageous over petroleum-derived polymers. There is much literature on proteins and carbohydrates derived from plants and animals and polyesters made from fermentation of plant material. The focus here is on proteins, which can be derived inexpensively from agricultural waste and have much versatility because of the various amino acid sequences found in nature. Keratin, wheat gluten, and egg albumin have been processed into films using a variety of techniques,[1–15] and these techniques include solvent-cast and thermally processed films. Solvent casting is tedious and the use of volatile organic compounds would defeat the purpose of environmental-friendliness. Thermal processing is simpler and the method currently embraced by the polymer industry. If proteins from sustainable resources are to be used commercially, the proteins have to be processed through preferred processing methods.

Naturally derived polymers suffer from several deficiencies such as instability over time and susceptibility to plasticization by water. For these polymers to be viable commercially, these inadequacies need to be overcome. Proteins afford several functional groups depending on the amino acid sequence including amide, acid, thiol, hydroxyl, and ring groups. Therefore, it is possible to chemically modify proteins at preferred sites to alter the properties.

Biochemically, transition metals are not spherically symmetrical with respect to charge and show directed valences, creating the ability to complex with protein ligands. The alkaline earth metals are spherically symmetrical with respect to charge and therefore usually do not complex effectively.[16] Therefore, it should be possible to complex transition metals with agricultural proteins to elicit beneficial properties, specifically, to bind sites on the protein with divalent transition metal ions to induce network formation or crosslinking.

The amino acid composition of wheat gluten, feather keratin, and egg albumin are different.[17,18] Most notably, feather keratin has about 7% cysteine, egg albumin has about 2% cysteine, and wheat gluten has about 2.5% cysteine. Wheat gluten is an amorphous protein obtained from wheat. Egg albumin is the major protein fraction of egg whites and is semicrystalline. Feather keratin is a semicrystalline protein too.[19,20] Wheat gluten can be deformed to high levels compared to egg albumin and feather keratin but the latter two proteins are much stiffer

Mention of trade names or commercial products in this article is solely for the purpose of providing specific information and does not imply recommendation or endorsement by the U.S. Department of Agriculture.

**Present address:* Biological Systems Engineering Department, Virginia Tech, Blacksburg, Virginia 24061.
Correspondence to: J. R. Barone (jbarone@vt.edu).

TABLE I
Blending Schemes

Scheme	Protein (%)	Glycerol (%)	H_2O (%)	Na_2SO_3 (%)	M^{2+} (%)
1	60	20	18	2	0
2	60	20	14	2	4
3	60	20	20	0	0
4	60	20	16	0	4

Protein is wheat gluten, egg albumin, or feather keratin; H_2O is deionized; M^{2+} refers to Cu^{2+}, Zn^{2+}, Mn^{2+}, or Ca^{2+}.

because of the crystallinity.[21] In addition, the latter proteins have a reduced permeability to water over wheat gluten as crystals act as impediments to diffusion and these proteins have more hydrophobic amino acids.[21] Therefore, methods to increase the properties of agricultural proteins are sought that are inexpensive, easy, and can be implemented using standard polymer processing techniques. Complexation with divalent transition metal ions could be such a method.

In this study, wheat gluten, egg albumin, and feather keratin were blended with glycerol and aqueous solutions of divalent metal ions. Stiffness was characterized in uniaxial tension as a function of type and amount of divalent metal ion. Permeability experiments were performed to note divalent metal ion effects on water and oxygen transport across protein/metal ion films. Network formation was assessed with birefringence and differential scanning calorimetry (DSC) experiments. Fourier transform infrared (FTIR) spectroscopy was used to assess possible network formation at specific chemical sites.

EXPERIMENTAL

Proteins

Feather keratin (M_w = 10,500 g/mol of reduced keratin, pI = 5.6) was obtained from Featherfiber® Corporation (Nixa, MO) and ground and sieved using a procedure described previously.[6–8] Wheat gluten (mixed gliadin and glutenin fractions, average reduced $M_w \approx$ 55,000 g/mol, pI = 7.5) and Type II egg albumin (M_w = 45,000 g/mol reduced egg albumin, pI = 4.5) were obtained in powder form from Aldrich Chemical.[8,22]

Preparation of blends

The proteins were blended with reagent grade glycerol (mol wt = 92.1 g/mol, boiling point = 290°C, density = 1.26 g/cm^3) obtained from Aldrich Chemical. Divalent metal ions were obtained from solutions of reagent grade copper sulfate ($CuSO_4$, mol wt = 159.6 g/mol), zinc sulfate ($ZnSO_4$, mol wt = 61.4 g/mol), and calcium chloride ($CaCl_2$, mol wt = 111.0 g/mol) all obtained from Fisher Scientific. Two types of blends were prepared: with and without reagent grade sodium sulfite (Na_2SO_3, mol wt = 126.0 g/mol, density = 2.63 g/cm^3) as a processing aid, also obtained from Fisher Scientific. Sodium sulfite was able to reduce sulfur–sulfur or cystine bonds and allow for easier polymer film formation.[7,11,12,21] The pH of the blends was pH = 8.9. For comparison of different proteins and ions, the blending schemes used are included in Table I showing relative mass percentages of each component. To compare the effect of various levels of zinc sulfate on egg albumin, the blending schemes are shown in Table II. There were practical limitations to dissolving sodium sulfite (about 1 : 3) and zinc sulfate (about 1 : 5) in deionized water so higher concentrations were not possible in this scheme.

Each blend was mixed on a Brabender mixing head at 40°C and 50 rpm for 15 min. The total material was 40 g and occupied 70% of the volume of the mixer. Following mixing, 5 g of sample was sandwiched between Teflon-coated aluminum foil and pressed into films in a Carver Press Autofour/30 Model 4394 at 140°C, 88964 N for 2 min. Most of the water was lost following processing as determined by weight measurements on the films. All of the films obtained were relatively clear but had a whitish hue to them when blended with $ZnSO_4$ and a bluish hue when blended with $CuSO_4$.

Mechanical testing of films

Test samples were prepared according to ASTM D882 for thin plastic films. The samples were 2.54-cm wide by 10.16-cm long and a 5.08-cm gage length

TABLE II
Blending Schemes for Egg Albumin-Zn^{2+}

Egg albumin	Glycerol	H_2O	Na_2SO_3	$ZnSO_4$
60 (0.00053)	20 (0.08686)	18 (0.40)	2 (0.00635)	0 (0)
60 (0.00053)	20 (0.08686)	16 (0.36)	2 (0.00635)	2 (0.0050)
60 (0.00053)	20 (0.08686)	14 (0.31)	2 (0.00635)	4 (0.0100)
60 (0.00053)	20 (0.08686)	12 (0.27)	2 (0.00635)	6 (0.0148)

H_2O is deionized.
Molar amounts are given in parentheses.

was employed. All films were of similar thickness of 0.040 ± 0.005 cm as measured with a digital micrometer. Mechanical testing of the films was performed at a crosshead speed of 2.54 cm/min using a Com-Ten Industries 95 RC Test System. A minimum of 15 films were tested and results reported as average values with standard deviations given.

Birefringence

During tensile testing, films were observed between crossed polarizers oriented at 45°C to the gage length (or tensile axis), using a white light source. Retardance was observed as color development in the sample. Although it was possible to convert retardance to birefringence values, all of the films were of the same thickness and therefore retardance was suitable for comparison.[23,24]

Permeability testing of films

Oxygen transmission rates (OTR) of films were measured following ASTM D3985-95. Film samples 6 cm × 6 cm were cut for oxygen permeability (OP) testing and average thickness was calculated from three measurements of each sample using a digital micrometer. OTRs were determined with an Oxtran 2/20 (Mocon, Minneapolis, MN). Samples were placed between two stainless steel plates with an opening 5 cm in diameter. Testing conditions were 50% humidity at 25°C. The test gas was set to 100% oxygen. OP was calculated by multiplying the measured OTR of each sample by its average thickness.

Following the ASTM E96-95, water vapor transmission rate (WVTR) was measured for each film and used to calculate water vapor permeability (WVP). Samples of films were cut into 6 cm by 6 cm pieces and average film thickness was calculated from three measurements using a digital micrometer. Film samples were placed inside permeability cups with a testing area 5 cm in diameter. A test solution of distilled-deionized water was placed inside the cup to form a high relative humidity environment (80–100% RH). To promote mass transfer through the films, the permeability cups were placed in a chamber with 0% RH (Drierite) with air circulation. Because films made from agricultural proteins were only moderate moisture barriers, a humidity-gradient formed inside the permeability testing cups between the surface of the test solution and the underside of the film samples. A modification to the ASTM method described by McHugh et al.[25] accounted for this gradient in the calculation of WVP. The initial weight of each cup was taken and then weight was measured at intervals that were at least three hours long over a period of 24 hours. Linear regression of time and weight data was used to calculate WVTR.

DSC

Thermal properties were assessed using a TA Instruments 910s Differential Scanning Calorimeter under nitrogen atmosphere. Samples were between 4 and 5 mg and small pinholes were punched into the lids to allow water to escape. One heating cycle was employed from 0°C to 320°C at a heating rate of 10°C/min according to ASTM D3417. The assignment of peaks and integration of peak areas was performed according to ASTM D3418. Using a two step heating cycle to first eliminate the large water or denaturation peak around 100°C will show the glass transition temperature (T_g) of wheat gluten which appears at around 167°C. The first step proceeds from 0°C to 160°C followed by a cooling step to 30°C then a second heating step to 320°C. Egg albumin and feather keratin do not show any features in this temperature range.

FTIR spectroscopy

FTIR analysis was performed with a Thermo Nicolet Avatar 370 in attenuated total reflectance (ATR) mode with a 45° ZnSe crystal. Pressure was applied to each film to ensure good polymer/crystal contact. A resolution of 4 cm^{-1} was used over 64 scans. Background spectra were obtained before each experiment and data plotted as absorbance so quantitative interpretations were possible.

RESULTS AND DISCUSSION

Mechanical properties

Figure 1 shows a bar graph comparing egg albumin (EA) samples made using Scheme 1, EA(1), and Scheme 2, EA(2), using Zn^{2+}, Cu^{2+}, and Ca^{2+}. A clear increase of the elastic modulus from about 0.08 GPa to 0.16 GPa upon the addition of 4 wt% $CuSO_4$ or $ZnSO_4$ was observed. No such increase was observed with $CaCl_2$ addition. The clarity of the films and uniform thicknesses observed seemed to indicate that the metal compounds were not interfering with film formation although they did impart a hue to the films. Using Scheme 3, EA(3), and Scheme 4, EA(4), showed a similar trend to Schemes 1 and 2, indicating that sodium sulfite was not affecting any protein-transition metal ion interaction. It was observed that egg albumin blended without sodium sulfite yielded an elastic modulus of about half of the egg albumin blended with sodium sulfite. This may indicate that sodium sulfite reduces sulfur-sulfur bonds to lower viscosity during processing, then re-forms (oxidizes) more inter-molecular sulfur-sulfur than prior to reduction, thus increasing elastic modulus.[7,11,12,21] However, upon addition of divalent transition metal ions, any effects from cystine bond reformation were

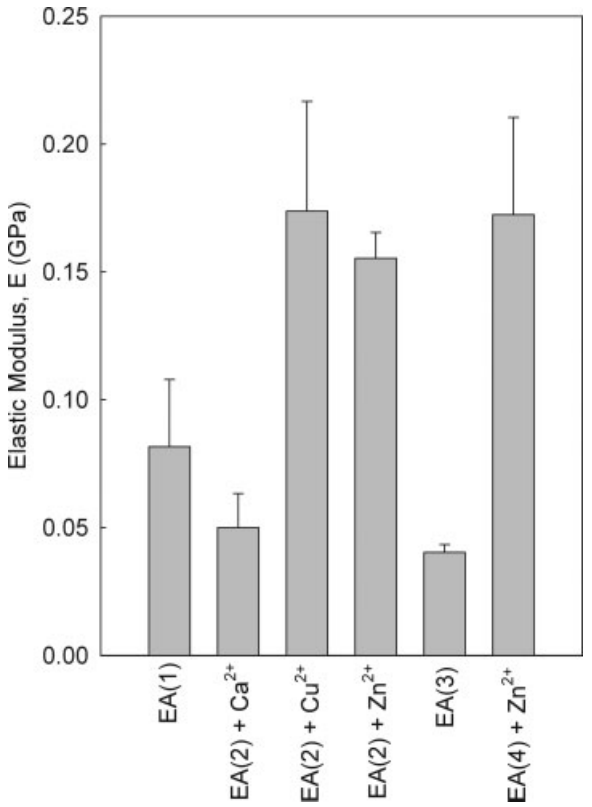

Figure 1 Egg albumin (EA) blended with various divalent metal ions. Numbers in parentheses refer to blending schemes outlined in Table I.

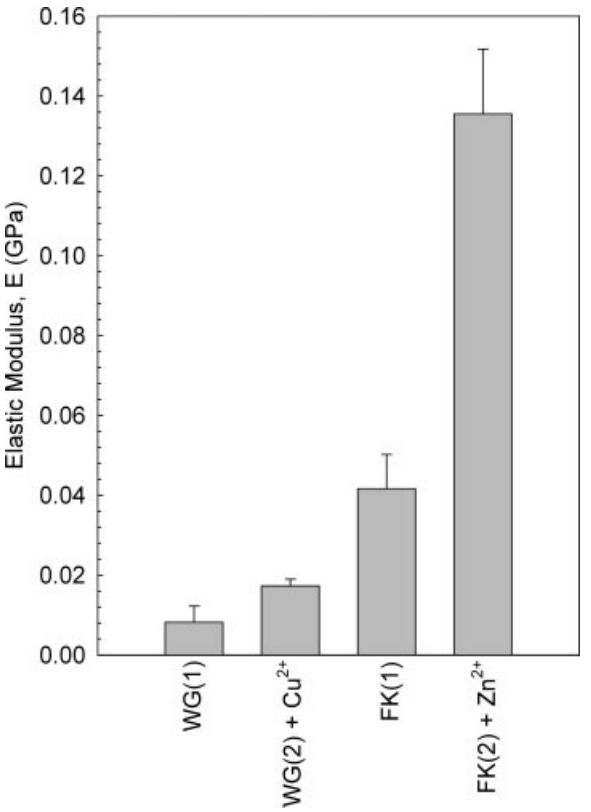

Figure 2 Wheat gluten (WG) and feather keratin (FK) blended with divalent transition metal ions. Numbers in parentheses refer to blending schemes outlined in Table I.

outweighed by metal ion binding as observed through comparison of EA(2)+Zn^{2+} and EA(4)+Zn^{2+}. Figure 2 shows the stiffness increase of wheat gluten blended with 4 wt% $CuSO_4$ and feather keratin blended with 4 wt% $ZnSO_4$. Again, the elastic modulus increased by 2 times for wheat gluten and over 3 times for feather keratin. The feather keratin may experience a larger increase because of the larger amount of cysteine in the protein and the fact that zinc will chelate cystine. This is in addition to reduction and oxidation of cystine by the sodium sulfite contributing as described previously.

Figure 3 shows the increase in elastic modulus and concurrent decrease in strain to break for egg albumin with varying $ZnSO_4$ content. The stiffness again continuously increased to almost 4 times its original value as more zinc sulfate was added. The protein materials without divalent transition metal ions have elastic moduli that are similar to other natural polymeric materials but that are about an order of magnitude lower than commercial semi-crystalline polyolefins that comprise many synthetic polymer applications. The protein materials with divalent transition metal ions have elastic moduli that are still lower than high volume semi-crystalline polyolefins and that more resemble mostly amorphous polyolefins or rubbery thermoplastic materials.

Permeability

For similarly thick egg albumin films, water vapor permeability decreased from 13.63 to 9.00 g mm/kPa^{-1}

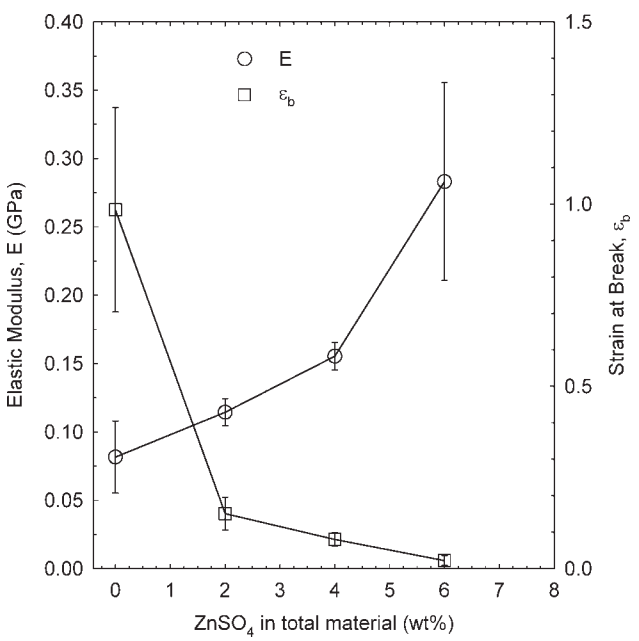

Figure 3 Egg albumin blended with increasing amounts of $ZnSO_4$. Blending procedures are outlined in Table II.

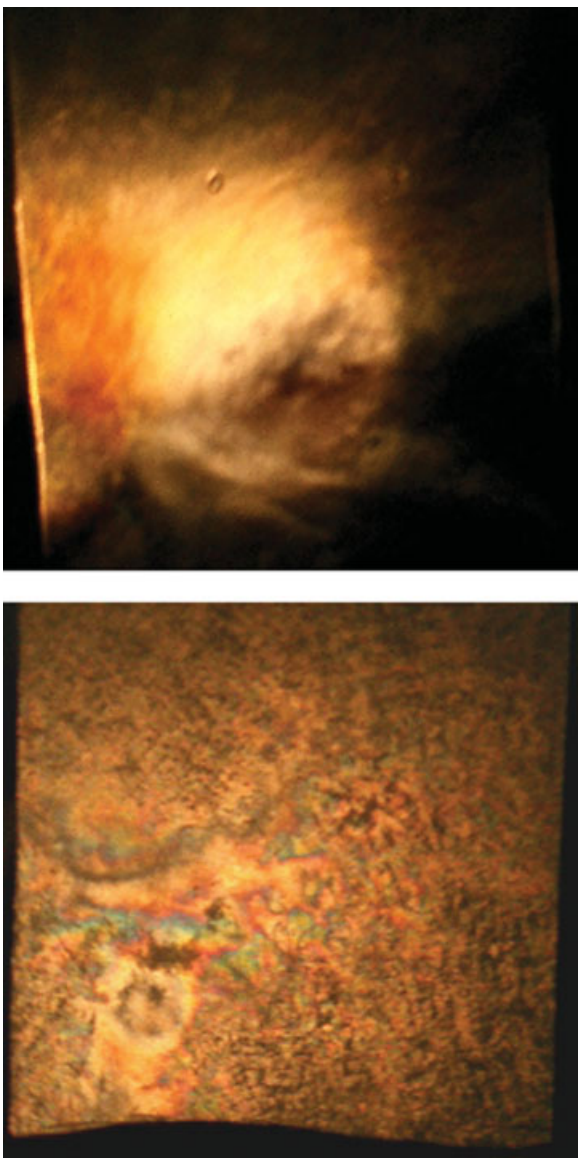

Figure 4 Initial retardance states of egg albumin with (a) no $ZnSO_4$ and (b) with 4 wt% $ZnSO_4$ blended according to schemes 3 and 4 in Table II. [Color figure can be viewed in the online issue, which is available at www.interscience.wiley.com.]

h^{-1} m^{-2} upon addition of 4 wt % $ZnSO_4$. However, OP was fairly constant with 22.70 cc μm m^{-2} day kPa for egg albumin control and 22.55 cc μm m^{-2} day kPa for egg albumin with 4 wt% $ZnSO_4$. Network formation would be consistent with the lower water vapor permeability although oxygen still has a suitable pathway through the film. The difference could be related to the size of a water molecule versus an oxygen molecule. The void space within the protein film could have been reduced just enough with the addition of Zn^{2+} to exclude water but not enough to exclude oxygen. However, water has an affinity for itself that oxygen does not, and so once inside the film, water may resaturate with other water molecules and with available sites, such as hydroxyls, on the protein. Oxygen would not be expected to do this.

Birefringence

Figure 4 shows a comparison between the initial retardance of an egg albumin sample prepared according to Scheme 3 [Fig. 4(a)] and an egg albumin sample with $ZnSO_4$ prepared according to Scheme 4 [Fig. 4(b)] in Table I. Both show a finite amount of initial retardance indicating that some ''structure'' has developed in each following blend-

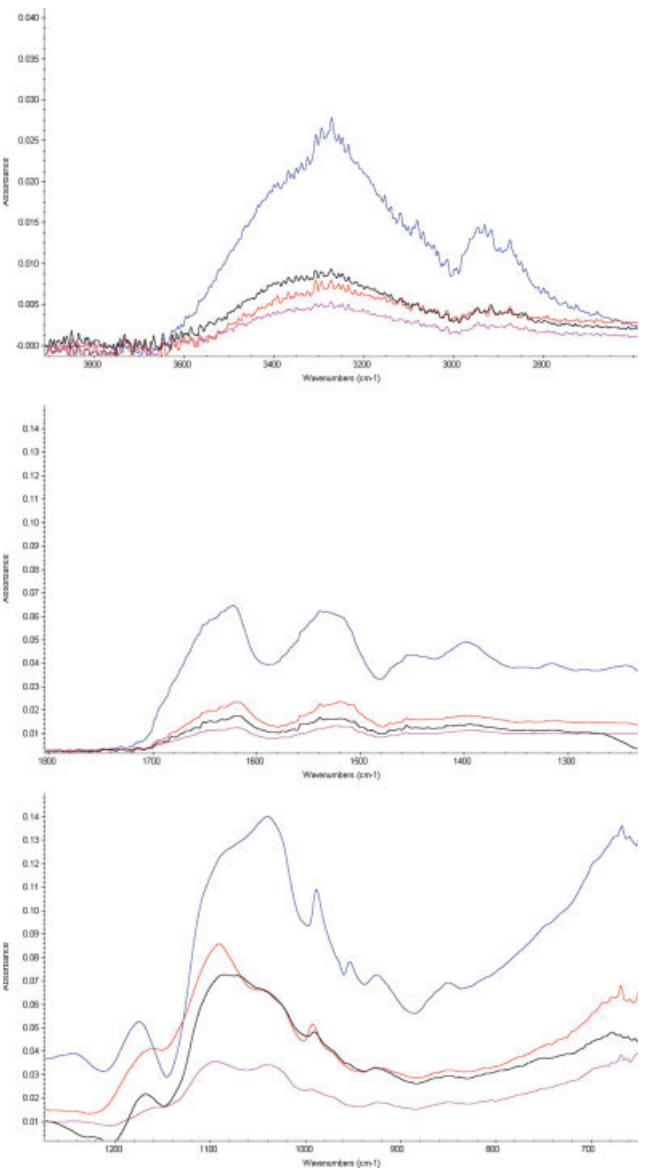

Figure 5 FTIR spectra of egg albumin-Zn blends (a) centered at 3300 cm^{-1}, (b) in Amide I, II, and III regions, (c) in 1200–800 cm^{-1} region. Blue = 0% Zn^{2+}, Black = 2% Zn^{2+}, Pink = 4% Zn^{2+}, Red = 6% Zn^{2+}. [Color figure can be viewed in the online issue, which is available at www.interscience.wiley.com.]

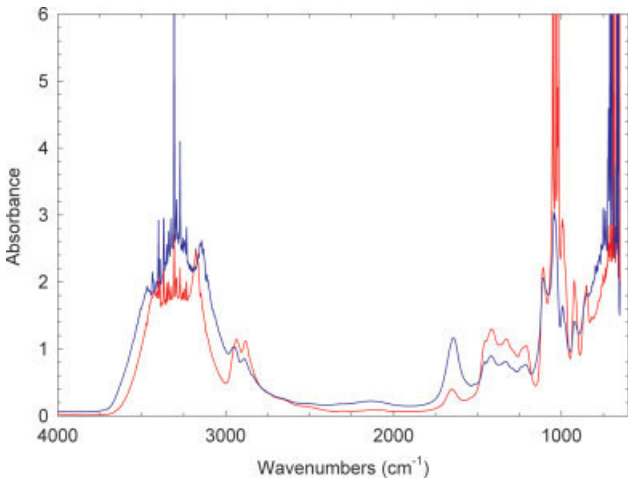

Figure 6 FTIR spectra of glycerol and a 20 : 16 : 4 parts by weight of glycerol : de-ionized H_2O : $CuSO_4$. [Color figure can be viewed in the online issue, which is available at www.interscience.wiley.com.]

ing and processing. However, the initial retardance shown in Figure 4(b) is clearly different from that in Figure 4(a). The polymer with no Zn^{2+} ions had large isolated areas of high retardance indicated by the red regions and areas of low retardance indicated by the yellow regions. Dark regions in the light path indicate no retardance. The polymer with Zn^{2+} ions showed a much different retardance pattern. The EA sample with Zn^{2+} had very small regions of red, blue, and green interdispersed throughout the sample. Blue and green were the highest retardance values before going through the first order of retardance. Adding divalent transition metal ions adds a new element of structure to the polymer. The retardance data seems to suggest a continuous network formed in the egg albumin with the addition of Zn^{2+}.

FTIR

Figure 5(a) shows the amide region of the egg albumin/Zn^{2+} blends at around 3300 cm^{-1}.[20,26–28] A reduction in this peak indicated that amide may be bound and therefore could not vibrate as freely as a polymer without divalent transition metal ions. A portion of this peak originated from glycerol and therefore glycerol may be bound by the zinc ions as well. Figure 5(b) shows the Amides I, II, and III regions of the egg albumin spectrum. Amide I shifts about 5 wavenumbers to lower values with the addition of zinc ions but the Amide II peak shifts 15 wavenumbers to lower values. This may indicate increased binding at amide sites over carbonyl sites. The Amide II peak was consistent with a β-sheet structure, a structure that was observed to dominate after processing the protein.[7,28] The Amide III peak at 1245 cm^{-1} disappeared with the addition of zinc ions. Figure 5(c) shows the peak at 1175 cm^{-1}, which was assigned to a C—C stretching mode.[20,26–28] This peak diminished and shifted about 10 wavenumbers to lower frequency with the addition of zinc ions. The strong peak at 1100 cm^{-1} originated in glycerol and a clear reduction and shift in this peak to much higher frequency was observed upon addition of zinc ions. Upon addition of 2 wt % of zinc ions to egg albumin, there was a large decrease in the FTIR peak intensities characteristic of the protein. Further addition of zinc ions resulted in modest peak intensity decrease. At 2 wt % $ZnSO_4$ relative to egg albumin, there were 9 mol of $ZnSO_4$ to egg albumin. Addition of 4 and 6 wt % $ZnSO_4$ to egg albumin resulted in 18 and 27 mol of $ZnSO_4$, respectively, relative to egg albumin. Clearly, a low amount of binding sites are needed to get large stiffness increases in the protein. Binding appears to maximize at about 9–18 divalent transition metal ions per egg albumin molecule.

Figure 6(a) shows FTIR spectra of glycerol and a mixture of glycerol : deionized H_2O : $CuSO_4$ at 20 : 16 : 4 parts by weight (the same ratio used in some of the protein blends). The CH_2-axisymmetric (2935 cm^{-1}) and CH_2-symmetric (2882 cm^{-1}) stretching regions shift to higher wavenumbers with the addition of copper ions. However, three peaks at 1052, 1035, and 1010 cm^{-1}, representing the three distinct —OH peaks on glycerol disappear with the addition of copper ions. The FTIR results for the Cu^{2+}/glycerol solution again indicate glycerol binding to the copper ions even without the protein.

DSC

In DSC experiments on native proteins, melting points appeared at about 250°C for semicrystalline

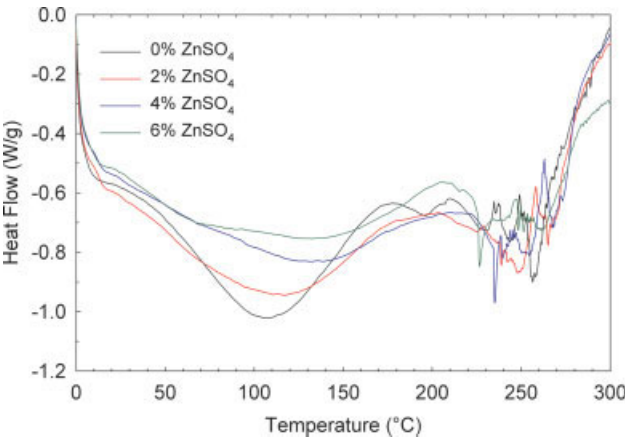

Figure 7 DSC data of egg albumin-Zn blends. [Color figure can be viewed in the online issue, which is available at www.interscience.wiley.com.]

proteins with degradation occurring at subsequent temperatures.[19,20] DSC experiments with protein–glycerol blends typically showed two major phenomena: a peak due to evaporation of water at about 100°C and a peak due to evaporation of glycerol at about 250°C. The addition of glycerol shifted the water or denaturation peak to higher temperatures.[6] The evaporation of glycerol was much more pronounced and therefore hid any potential crystallinity in the protein–glycerol blends. DSC experiments on protein-glycerol and divalent transition metal ion blends showed several changes to the thermal behavior of protein–glycerol blends. First, the denaturation peak increasingly shifted to higher temperatures and became shallower as more Zn^{2+} was added to egg albumin as shown in Figure 7. This would be consistent with a binding mechanism, making it more difficult for glycerol to detach from the protein. Previously, an intermediate peak around 200°C for the 0% Zn^{2+} sample was assigned to a new crystalline phase while higher temperature peaks were assigned to glycerol evaporation, with the highest at 255°C.[34] The intermediate crystalline peak disappeared with addition of Zn^{2+} ions or perhaps relocated to a higher temperature. However, glycerol release peaks appeared at higher temperatures (>255°C without Zn^{2+}) with the addition of Zn^{2+} ions, consistent with a binding mechanism, and the behavior observed in the ''denaturation'' peak at lower temperatures.

Structure

All experiments were conducted at pH = 8.9. For each protein, pH > pI resulting in an overall negative charge on the protein. This made it possible to bind sites on one protein with sites on another protein using divalent transition metal ions. Several binding mechanisms appear dominant in the proteins. In egg albumin, reduction of the amide peak at 3300 cm^{-1}, a small shift in the Amide I peak and a larger shift in the Amide II peak, and large reductions and shifts in the glycerol peak at 1100 cm^{-1} indicated that the directed valence of the divalent transition metal ion was binding these sites in particular. The change in the C—C stretching vibration at 1175 cm^{-1} indicated a conformational change in the protein molecule with addition of zinc ions. Figure 8 shows a model of a possible binding scheme consistent with the FTIR data that would also explain the increased elastic modulus and reduced evaporation of glycerol. The Cu^{2+} ion associated with the O—H groups on glycerol. The peptide shown is just a sequence of simple amino acids. The Cu^{2+} ion associated with C=O, which had a partial negative charge, on the peptide. It also associated with N—H and C—H on the peptide. The glycerol-Cu^{2+} complex most probably had a stronger affinity for some C=O sites than for others. There was also affinity for Asp and Glu O=C—O sites. More specifically, the divalent transition metal ion had six directed binding sites, with hydroxyls on glycerol occupying three of them and amides, carbonyls, and CH groups on proteins occupying the other three. In the FTIR spectra, larger shifts in the glycerol peaks with addition of divalent transition metal ion indicated more hydroxyl binding to the ion than other groups. However, over the entire peptide, there were more amide groups bound to the divalent transition metal ion than carbonyls as indicated by the larger shift in amide peaks over carbonyls in FTIR.

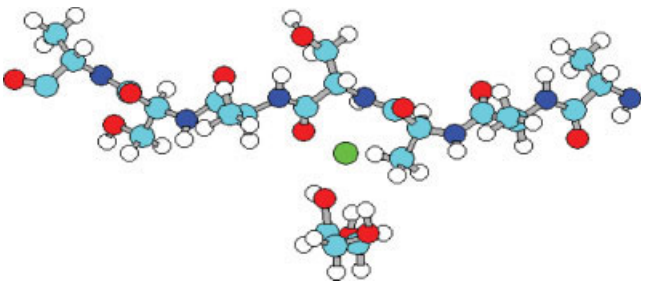

Figure 8 Three-dimensional model of possible binding mechanisms of divalent transition metal ion with glycerol and protein. Color code: Dark Blue = Nitrogen, Light Blue = Carbon, White = Hydrogen, Red = Oxygen, Green = Cu^{2+}. [Color figure can be viewed in the online issue, which is available at www.interscience.wiley.com.]

CONCLUSIONS

Proteins obtained from agricultural sources such as egg albumin, wheat gluten, and feather keratin represent a unique class of polymers that could be processed into value-added products. Binding divalent transition metal ions to the proteins binds amide and carbonyl sites on the protein and hydroxyl sites on the glycerol plasticizer. This created a highly bound network of protein-metal ion-glycerol exhibited physically by increased elastic modulus and decreased water permeability. FTIR and birefringence data confirmed a bound structure.

References

1. Yamauchi, K.; Yamauchi, A.; Kusunoki, T.; Kohda, A.; Konishi, Y. J Biomed Mater Res 1996, 31, 439.
2. Tanabe, T.; Okitsu, N.; Yamauchi, K. Mater Sci Eng C 2004, 24, 441.
3. Pavlath, A. E.; Houssard, C.; Camirand, W.; Robertson, G. H. Text Res J 1999, 69, 539.
4. Schrooyen, P. M. M.; Dijkstra, P. J.; Oberthur, R. C.; Bantjes, A.; Feijen, J. J Agric Food Chem 2000, 48, 4326.
5. Schrooyen, P. M. M.; Dijkstra, P. J.; Oberthur, R. C.; Bantjes, A.; Feijen, J. J Agric Food Chem 2001, 49, 221.

6. Barone, J. R.; Schmidt, W. F.; Liebner, C. F. J Appl Polym Sci 2005, 97, 1644.
7. Barone, J. R.; Schmidt, W. F.; Gregoire, N. T. J Appl Polym Sci 2006, 100, 1432.
8. Gennadios, A. Protein-Based Films and Coatings; CRC Press: Boca Raton, FL, 2002.
9. Sanchez, A. C.; Popineau, Y.; Mangavel, C.; Larre, C.; Gueguen, J. J Agric Food Chem 1998, 46, 4539.
10. Cuq, B.; Boutrot, F.; Redl, A.; Lullien-Pellerin, V. J Agric Food Chem 2000, 48, 2954.
11. Morel, M.-H.; Bonicel, J.; Micard, V.; Guilbert, S. J Agric Food Chem 2000, 48, 186.
12. Irissin-Mangata, J.; Baudin, G.; Boutevin, B.; Gontard, N. Eur Polym J 2001, 37, 1533.
13. Mangavel, C.; Barbot, J.; Gueguen, J.; Popineau, Y. J Agric Food Chem 2003, 51, 1447.
14. Woerdeman, D. L.; Veraverbeke, W. S.; Parnas, R. S.; Johnson, D.; Delcour, J. A.; Verpoest, I.; Plummer, C. J. G. Biomacromolecules 2004, 5, 1262.
15. Gallstedt, M.; Matttozzi, A.; Johansson, E.; Hedenqvist, M. S. Biomacromolecules 2004, 5, 2020.
16. Zubay, G. Biochemistry, W. C. Biochemistry; Zubay, G., Ed.; Brown Publishers: Dubuque, IA, 1993.
17. Fox, P. F.; Condon, J. J. Food Proteins; Applied Science Publishers: London, 1982.
18. Whitaker, J. R.; Tannenbaum, S. R. Food Proteins; AVI Publishing: Connecticut, 1977.
19. Schmidt, W. F.; Line, M. J. TAPPI Proc Nonwovens Conf 1996, 135.
20. Martinez-Hernandez, A. L.; Velascos-Santo, C.; de Icaza, M.; Castano, V. M. Int J Environ Pollut 2005, 23, 162.
21. Barone, J. R.; Dangaran, K; Schmidt, W. F. J Agric Food Chem 2006, 54, 5393.
22. Wu, Y. V.; Dimler, R. J. Arch Biochem Biophys 1963, 102, 230.
23. Fuller, G. G. Optical Rheometry of Complex Fluids; Oxford University Press: New York, 1995.
24. Carl Zeiss Corporation; Michel-Levy Chart: Thornwood, NY 2000.
25. McHugh, T. H.; Avena-Bustillos, R. J.; Krochta, J. M. J Food Sci 1993, 58, 899.
26. Edwards, H. G. M.; Hunt, D. E.; Sibley, M. G. Spectrochim Acta A 1998, 54, 745.
27. Pielesz, A.; Freeman, H. S.; Weselucha-Birczynska, A.; Wysocki, M.; Wlochowicz, A. J Mol Struct 2003, 651–653, 405.
28. Nishikawa, N.; Tanizawa, Y.; Tanaka, S.; Horiguchi, Y.; Asakura, T. Polymer 1998, 39, 3835.